Original Article

MOLECULAR METABOLISM

Inhibition of central *de novo* ceramide synthesis restores insulin signaling in hypothalamus and enhances β-cell function of obese Zucker rats

Mélanie Campana [1], Lara Bellini [1], Claude Rouch [1], Latif Rachdi [2], Nicolas Coant [1], Noémie Butin [3], Cécile L. Bandet [4], Erwann Philippe [1], Kelly Meneyrol [1], Nadim Kassis [1], Julien Dairou [5], Eric Hajduch [4], Benoit Colsch [3], Christophe Magnan [1], Hervé Le Stunff [1,6,*]

ABSTRACT

Objectives: Hypothalamic lipotoxicity has been shown to induce central insulin resistance and dysregulation of glucose homeostasis; nevertheless, elucidation of the regulatory mechanisms remains incomplete. Here, we aimed to determine the role of *de novo* ceramide synthesis in hypothalamus on the onset of central insulin resistance and the dysregulation of glucose homeostasis induced by obesity.

Methods: Hypothalamic GT1-7 neuronal cells were treated with palmitate. *De novo* ceramide synthesis was inhibited either by pharmacological (myriocin) or molecular (si-Serine Palmitoyl Transferase 2, siSPT2) approaches. Obese Zucker rats (OZR) were intracerebroventricularly infused with myriocin to inhibit *de novo* ceramide synthesis. Insulin resistance was determined by quantification of Akt phosphorylation. Ceramide levels were quantified either by a radioactive kinase assay or by mass spectrometry analysis. Glucose homeostasis were evaluated in myriocin-treated OZR. Basal and glucose-stimulated parasympathetic tonus was recorded in OZR. Insulin secretion from islets and β-cell mass was also determined.

Results: We show that palmitate impaired insulin signaling and increased ceramide levels in hypothalamic neuronal GT1-7 cells. In addition, the use of deuterated palmitic acid demonstrated that palmitate activated several enzymes of the *de novo* ceramide synthesis pathway in hypothalamic cells. Importantly, myriocin and siSPT2 treatment restored insulin signaling in palmitate-treated GT1-7 cells. Protein kinase C (PKC) inhibitor or a dominant-negative PKCζ also counteracted palmitate-induced insulin resistance. Interestingly, attenuating the increase in levels of hypothalamic ceramides with intracerebroventricular infusion of myriocin in OZR improved their hypothalamic insulin-sensitivity. Importantly, central myriocin treatment partially restored glucose tolerance in OZR. This latter effect is related to the restoration of glucose-stimulated insulin secretion and an increase in β-cell mass of OZR. Electrophysiological recordings also showed an improvement of glucose-stimulated parasympathetic nerve activity in OZR centrally treated with myriocin.

Conclusion: Our results highlight a key role of hypothalamic *de novo* ceramide synthesis in central insulin resistance installation and glucose homeostasis dysregulation associated with obesity.

© 2017 The Authors. Published by Elsevier GmbH. This is an open access article under the CC BY-NC-ND license (http://creativecommons.org/licenses/by-nc-nd/4.0/).

Keywords Ceramide; Lipotoxicity; Hypotalamus; Insulin resistance; Insulin secretion

1. INTRODUCTION

An increasing body of evidence shows that lipids control energy balance through their action on the hypothalamus [1,2]. Obesity following a high fat diet (HFD) but also intra-hypothalamic injections of saturated fatty acids (FFAs) have been shown to induce central lipotoxicity, evidenced by the deregulation of energy homeostasis [1,3]. Central lipotoxicity has also been shown to be deleterious for the hypothalamic control of glucose homeostasis [4,5]. Indeed, it is well established that in rodents fed with HFD, excessive lipid intake induces hypothalamic insulin resistance (IR) and decreases liver insulin sensitivity, resulting in increased liver glucose production [4,5].

[1]Sorbonne Paris Cité, Université Denis Diderot, Unité de Biologie Fonctionnelle et Adaptative, CNRS UMR 8251, Bâtiment Buffon, PO box 7126, 4, rue Marie-Andrée Lagroua Weill-Halle, 75205 Paris Cedex 13, France [2]INSERM U1016, Université Paris-Descartes, Institut Cochin, Paris, France [3]CEA, DRF, Institut Joliot, Service de Pharmacologie et d'Immunoanalyse, UMR 0496, Laboratoire d'Etude du Métabolisme des Médicaments, MetaboHUB, Université Paris Saclay, F-91191 Gif-sur-Yvette cedex, France [4]INSERM U1138, Centre de Recherche des Cordeliers, Paris, France [5]Laboratoire de Chimie et Biochimie Pharmacologique et Toxicologiques, Université Paris Descartes CNRS UMR 8601, Paris, France [6]Molecular Neuroendocrinology of Food intake, Neuroscience Paris-Saclay Institute (NeuroPSI), UMR 9197, Université Paris-Sud, France

*Corresponding author. Unité Biologie Fonctionnelle et Adaptative, CNRS UMR 8251, Équipe Régulation de la glycémie par le système nerveux central, Université Paris Diderot, Paris, France. E-mail: hlestunff62@gmail.com (H. Le Stunff).

Abbreviations: IR, insulin resistance; HFD, high fat diet; T2D, Type 2 diabetes mellitus; PKCs, proteins kinase C; ER, endoplasmic reticulum; CerS, ceramide Synthase; Thr-308, Threonine 308; Ser-473, Serine 473; DH-C_2-cer, dihydroceramide; d4-palmitate, Deuterium-labeled palmitate; SPT2, Serine-palmitoyl transferase 2; C_2-Cer, C_2-Ceramide; LZR, Lean Zucker rat; OZR, Obese Zucker rat; ICV, intracerebroventricular; M, myriocin

Received September 14, 2017 • Revision received October 17, 2017 • Accepted October 27, 2017 • Available online 7 November 2017

https://doi.org/10.1016/j.molmet.2017.10.013

 © 2017 The Authors. Published by Elsevier GmbH. This is an open access article under the CC BY-NC-ND license (http://creativecommons.org/licenses/by-nc-nd/4.0/).

Mechanisms of hypothalamic insulin resistance induced by central lipotoxicity are still not completely understood, although it has been demonstrated that β-oxidation of FFAs may be involved [5,6]. Indeed, inhibition of the hypothalamic carnitine palmitoyl transferase 1, which regulates FFA β-oxidation [7], improves hepatic insulin action [5,6]. We and others showed previously that HFD or palmitate activation of PKCθ in hypothalamus, leading to impairment of central insulin signaling [4,8] is associated with hepatic IR [4]. Studies have shown an increase in lipids such as ceramides and diacylglycerols in the hypothalami of mice fed with HFD, centrally infused with palmitate, and in obese Zucker rats (OZR) [4,9]. Interestingly, infusion of ceramide analogs in the hypothalamus has been shown to deregulate energy homeostasis by regulating ER stress [10,11].

Since ceramides have been linked to peripheral lipotoxicity, especially in the onset of IR [12,13], the aim of the present study was to decipher the role of endogenous ceramide synthesis on the deregulation of hypothalamic insulin signaling and its consequences on glucose homeostasis. We found that *de novo* ceramide synthesis induced a hypothalamic IR through the activation of PKCζ. Interestingly, we also found that inhibition of *de novo* ceramide synthesis in the hypothalami of OZR improved glucose tolerance. The inhibition of hypothalamic ceramide synthesis slightly improved peripheral insulin sensitivity in OZR. In contrast, central inhibition of *de novo* ceramide synthesis in OZR was correlated to an increase of pancreatic β-cell area and insulin secretion by activation of the parasympathetic nervous system.

2. MATERIAL AND METHODS

2.1. Materials

Tissue culture medium was from Gibco. [γ-^{32}P]ATP was purchased from PerkinElmer. Palmitate, fatty-acid-free BSA, MTT [3-(4,5-dimethylthiazol-2-yl)-2,5-diphenyl-2*H*-tetrazolium bromide], ethylenediamine-tetra-acetic acid (EDTA), disodium salt, perchloric acid, hydrogen chloride, Anti-HA (hemagglutinin), SPT2 antibodies, and insulin human solution were from Sigma—Aldrich. Myriocin, L-cycloserine, D609, C_2-ceramide, C_2-dihydroceramides, and N-butyldeoxynojirimycin were from Enzo Life Sciences. Ro31-8220 and DAG kinase were from Calbiochem. All solvents were from Merck Eurolab or Fisher Scientific. phospho-Akt (Thr 308), phospho-Akt (Ser 473), Akt, p-PKCζ (Thr 410-403), PKCζ, and β-actin antibodies were from Cell Signaling. Ultrapure water was obtained with a Milli-Q system (Millipore, Bedford, MA, USA). Adenoviruses containing the cDNA of GFP, wild-type PKCζ (WT- PKC), constitutive active PKCζ (CA-PKCζ), or kinase-dead PKCζ (KD-PKCζ) were prepared as previously described [14]. All PKCζ constructs contained an HA tag for monitoring their expression.

2.2. Cell culture

GT1-7 murine hypothalamic cells (kindly provided by the Dr. P. Mellon, UCSD, USA) were cultured in DMEM medium supplemented with 10% FBS and 100 U/mL penicillin/streptomycin [15]. Palmitate was conjugated with fatty acid-free BSA (molar ratio FFA/BSA was 5:1) and diluted in DMEM supplemented with 1% FBS to obtain a 0.5 or 1 mM final concentration. After palmitate treatment, cells were stimulated with insulin (100 nM) for 5 min.

2.3. Measurement of cell viability

Cells were treated with MTT (1 mg/ml) for 4 h. Supernatants were discarded, and DMSO was added. Absorbance was measured at 560 nm using a microplate reader (Dynex-MRX).

2.4. Implantation of intracerebroventricular (icv) cannulae and central treatments

Ten-weeks-old male obese Zucker rats (OZR; 300—350 g) and lean Zucker rats (LZR; 250—300 g) (Charles River) were used. The experimental protocol was approved by the institutional animal care and use committee of the Paris Diderot University (CEEA40). Chronic icv cannulae were implanted under isoflurane anesthesia, and animals received a 10 μg/kg i.p. administration of xylazine. They were then placed on a stereotaxic frame. A catheter tube was connected from the brain infusion cannulae to an osmotic minipump flow moderator (model 2004; Alzet, Rabalot, France). The minipump was inserted in a subcutaneous pocket on the dorsal surface of the animal, created using blunt dissection and connected through a catheter to a depth-adjustable cannula implanted on ICV (X:—0.8 mm; Y:—1.5 mm; Z:—3.5 mm). Specificity of the ICV injections was controlled as previously described [16]. Zucker rats were then chronically infused for 28 days with either (300 nM) myriocin or vehicle (NaCl 9‰). Myriocin (300 nM) was prepared in NaCl 9‰. In Wistar rats, either C2-ceramide or DH-C_2-ceramide or vehicle (DMSO 5%/NaCl 9‰) were acutely ICV injected and insulin signalling was determined after 2 h post-injection. C_2-ceramide/DH-C2-ceramide solution (25 nM) was prepared in 5% DMSO. The selection of these doses was based on previous reports [10]. Prior to sacrifice, animals received an injection of insulin (2 mUI) or saline icv using the cannulae. Animals were sacrificed after 5 min, and tissues were collected and immediately frozen.

2.5. Glucose and insulin tolerance tests

Fourteen and 21 days after stereotaxic surgery, blood glucose levels were measured after glucose administration (oral glucose tolerance test, OGTT) or insulin (insulin tolerance test, ITT), respectively, with a glucometer (Accucheck, Roche) in overnight-fasted rats. 0.75 UI/kg insulin (Actrapid, Novonordisk) via intra-peritoneal injection was used for ITT, and 2 g/Kg D-glucose (Sigma—Aldrich) was administered orally via gavage for OGTT. During OGTT, blood samples were collected from the tail, and plasma was extracted and stored at −80 °C before further analysis. Insulin concentration was evaluated using ELISA methods (Rat Insulin Elisa, ALPCO, Eurobio, Courtaboeuf, France).

2.6. Western blotting

Cells lysates were obtained and analyzed by immunoblotting, as described [17]. A list of the antibodies used is shown in Supplementary Table 1.

2.7. Measurement of ceramide levels

Ceramide levels were measured by the diacylglycerol (DAG) kinase enzymatic method as previously described [17]. Briefly, lipid extracts were incubated in the presence of *E. coli* DAG kinase and [γ-^{32}P]-ATP. Reaction was stopped, and [γ-^{32}P]-ceramide phosphate was resolved by TLC with chloroform/acetone/methanol/acetic acid/water (10:4:3:2:1, by vol.) and quantified using a FLA700 PhosphorImager (GE Healthcare). An aliquot was used to quantify total phospholipid levels as described previously [18]. Ceramide levels are expressed in pmol per nmol of phospholipids (PL) levels.

2.8. *In vitro* insulin secretion from isolated islets

Rats were anesthetized with pentobarbital. Islets of Langerhans were isolated after collagenase digestion of the pancreas as previously described [19]. *In vitro* insulin release was assayed on islet after overnight culture. Floating Islets were pre-incubated in KRBH-0.05% BSA with 2.8 mM of glucose for 30 min, followed by 60 min

 © 2017 The Authors. Published by Elsevier GmbH. This is an open access article under the CC BY-NC-ND license (http://creativecommons.org/licenses/by-nc-nd/4.0/).

incubation in KRBH-0.05% BSA with 2.8 or 16.7 mM glucose to measure glucose-induced insulin secretion. The supernatant was stored at −20 °C until assayed for insulin by ELISA (EUROBIO). Islets were homogenized in protein extraction buffer and stored until insulin determination.

2.9. Real-time PCR

RNA isolation, cDNA synthesis, and mRNA quantitation were carried out as described [17]. A list of the primer sequences is shown in Supplementary Table 2.

2.10. Parasympathetic firing-rate recordings

Firing-rate activities were recorded at the thoracic branch levels of the vagus nerve (parasympathetic) along the carotid artery in overnight-fasted rats as described previously [19].

Briefly, parasympathetic nerves were placed on a pair of recording silver wire electrodes (0.6-mm diameter), and action potentials were displayed and saved on a computer after initial amplification through a low-noise amplifier (Bio Amp, ADInstruments). Unipolar nerve activity was recorded continuously during 15 min (baseline) and then 15 min after glucose injection (ip, 3 g/kg). Data were digitized with digitizer PowerLab/4sp. Signals were amplified 105 and filtered at low- and high-frequency cut-offs of 100 and 1,000 Hz and monitored with Chart 4 program (ADInstruments).

2.11. Lipidomics

Total lipid species were extracted according to the method of Folch et al. [20]. Ceramide lipid species were enriched in the lower phase (organic phase) and analyzed using an untargeted lipidomic approach by liquid chromatography coupled with high-resolution mass spectrometry (LC—HRMS) as described by Seyer et al. [21].

2.12. β-Cell area quantification

β-cell area from isolated, complete pancreata of Zucker rats was quantified as described previously [22]. Briefly, isolated pancreata were fixed in 10% buffered formalin, embedded and processed for immunohistochemistry using a previously described protocol [23] using mouse anti-insulin antibody (1:2,000; Sigma) and secondary antibodies (1:400 Donkey anti mouse HRP, Jackson ImmunoResearch). At 100 micron intervals that covered whole pancreas, give, longitudinal sections were imaged per pancreas. Slides were scanned using the Panoramic 250 Flash II scanner (3DHISTECH, Budapest, Hungary). Images were analyzed for β-cell area and the pancreatic area using inForm Tissue Finder software (PerkinElmer).

2.13. Plasma analysis

Enzyme assay kits were used to determine plasma FFAs (NEFA-C test, Wako, Frankfurt, Germany) and triglycerides concentrations (Boehringer-Mannheim, Ulm, Germany).

2.14. Measurement of plasma FFA levels by gas chromatography-mass spectrometry

Saturated and unsaturated FFA plasma levels were determined by GC—MS adapted from Araujo et al. [24]. Briefly, 50 μL of plasma were mixed with BF3 (14%)/methanol and 10 μg of heptadecanoic acid as an internal standard were added. Samples were heated (100 °C; 40 min) then cooled at room temperature. Heptane/distilled water (1:2) was added, samples were vortexed for 30 s, and then centrifuged for 2 min at 3000 rpm. The supernatant was collected and evaporated with a Speedvac (Jouan, Saint-Herblain, France). Dry samples were solubilized in heptane. One μL FA methyl esters (FAMEs) was analyzed on GC—MS instrument: with 1/100 split wherein a Shimadzu was interfaced with a GC2010 mass selective detector. The mass spectra and retention indices registered in the FAMEs GC/MS library were obtained using the Shimadzu GCMS-QP2010. This was done using the SLB-5 ms and the Supelcowax-10 columns (length 30 m × inner diameter 0.25 mm × film thickness 0.25 μm) made by Sigma—Aldrich Supelco (Lizy sur Ourcq, France).

2.15. Statistical analysis

Data are expressed as mean values ± S.E.M. Statistical significance was determined by Student's t-test when two groups were compared or ANOVA and Bonferroni post-hoc two-tailed test when more than two groups were compared. p value < 0.05 was considered significant.

3. RESULTS

3.1. Hypothalamic *de novo* ceramide synthesis induces central insulin resistance in obese Zucker rats

Obese Zucker rats (OZR) had a two-fold increase in total ceramide levels in hypothalamus (Figure 1A) and plasma (Table 1) compared to Lean Zucker rats (LZR). Intracerebroventricular (icv) infusion of myriocin (M), a potent inhibitor of serine palmitoyl-transferase (SPT), the rate limiting enzyme of *de novo* ceramide synthesis, inhibited the accumulation of ceramide in the hypothalamus of OZR compared to LZR (Figure 1A). Importantly, this central treatment with myriocin did not reduce circulating ceramides (Table 1), suggesting that myriocin is not mediating its effect by regulating peripheral action of ceramides. Ceramide accumulation in OZR was not associated with regulation of genes encoding enzymes of the *de novo* ceramide synthesis pathway, except for ceramide synthase 3, which was significantly down-regulated in OZR compared to LZR (Figure 1B). Central myriocin treatment did not affect body weight, food intake, or lean and fat body mass in either OZR or LZR (Table 1). However, myriocin treatment slightly reduced blood glucose and increased insulin levels in OZR. Circulating fatty acids and triglycerides levels were decreased in OZR (Table 1), reflecting an improvement in lipid homeostasis in these rats. In the hypothalamus of OZR animals, as previously shown [25]. Insulin was unable to increase phosphorylation of Akt (Figure 1C), which resulted in a 70% decrease of insulin response compared to LZR (Figure 1D). Interestingly, myriocin did not affect Akt phosphorylation in response to insulin in LZR, while it enabled insulin to phosphorylate Akt in OZR (Figure 1C), which recovered an insulin response similar to LZR (Figure 1D). The results suggest that *de novo* ceramide synthesis is involved in the onset of an IR state in hypothalamus of OZR.

3.2. C_2-ceramide induces hypothalamic insulin resistance both *in vivo* and *in vitro*

An acute icv treatment with an analog of ceramide, C_2-ceramide (C2-cer), in Wistar rats completely impaired Akt phosphorylation upon insulin stimulation in the hypothalamus, whereas dihydro-ceramide (DH-C_2-cer), its inactive analog [26], had no effects (Figure 1E,F). C_2-ceramide increased long chain ceramide content in a dose-dependent manner in hypothalamic neuronal GT1-7 cells (Figure 2A) without any effect on cell survival (Figure S1A). Accumulation of long chain ceramides was observed after 2 h of incubation (Figure 2B). Interestingly, C_2-cer inhibited insulin-stimulated Akt phosphorylation in a dose-dependent manner (Figure 2C,D). In contrast, DH-C_2-cer, did not impair insulin induced-Akt phosphorylation (Figure 2E,F). Our results suggest that ceramides play a direct role in the installation of an IR state in the hypothalamus *in vivo* and *in vitro*.

 © 2017 The Authors. Published by Elsevier GmbH. This is an open access article under the CC BY-NC-ND license (http://creativecommons.org/licenses/by-nc-nd/4.0/).

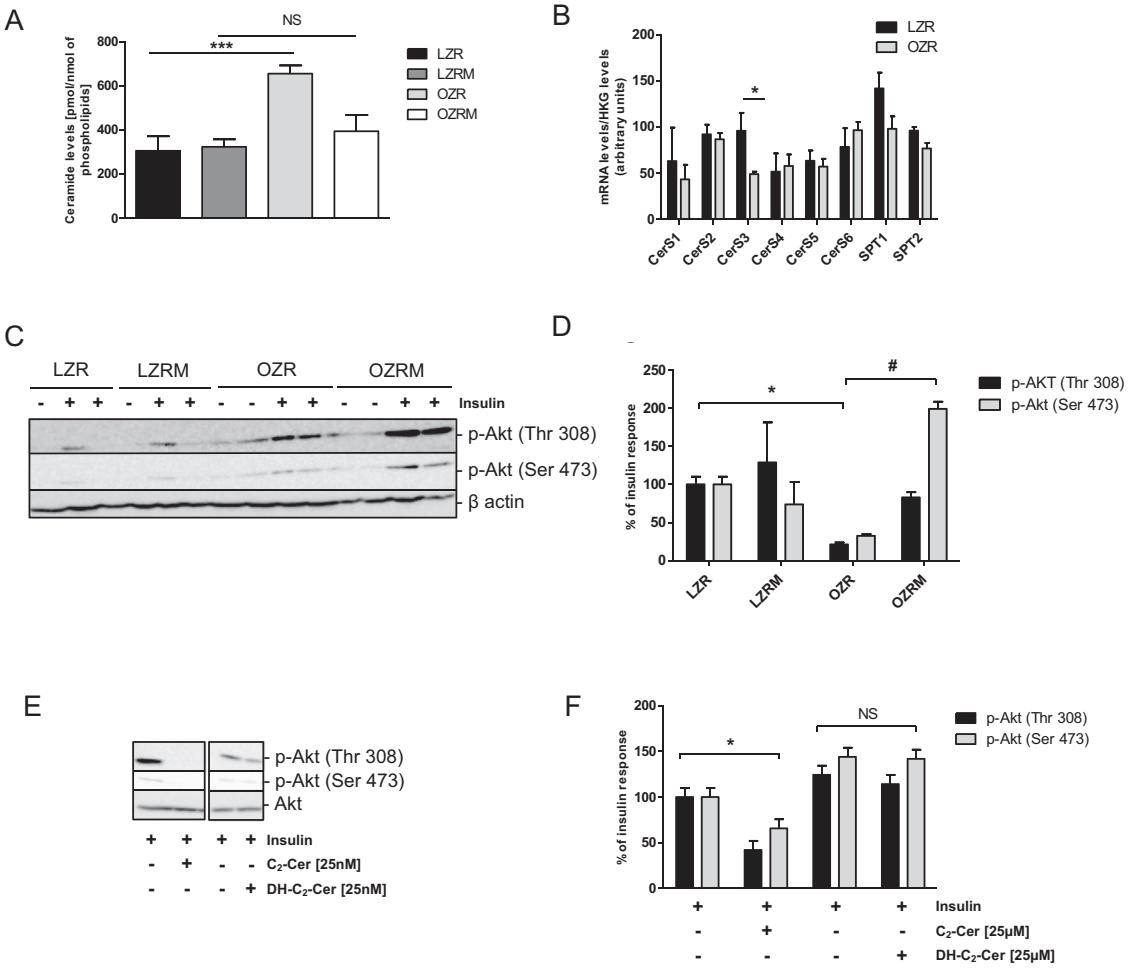

Figure 1: Effect of hypothalamic ceramide metabolism on insulin resistance in rats. (A-B-C-D) Zucker lean and obese rats were injected icv by mini pump with 300 nM of myriocin (LZRM, OZRM) or NaCl 9‰ (LZR, OZR) during 28 days. Before sacrifice, 2 mUI of insulin or NaCl were injected icv during 5 min. Hypothalami were collected and (A) ceramide levels, (B) mRNA expression levels and (C) and Akt phosphorylation were determined as described in Materials and Methods. (D) Percentage of insulin response on Akt phosphorylation of each animal groups. (E-F) Wistar rats were flash injected icv by stereotactic surgery with 25 nM of C_2-Ceramides, DH-C_2-Ceramides or saline solution. After 2 h, 10 UI of insulin were injected in saphenous vein, and animals were sacrificed 15 min later. Hypothalami were collected and intracellular ceramide content and phospho-Akt levels were determined. Error bars represent SEM; n = 3 animals per experimental group. *p < 0.05 C_2-Ceramide versus saline. Error bars represent SEM; n = 6–8 animals per experimental group. *p < 0.05, ***p < 0.001 LZR versus OZR, #p < 0.05 OZR versus OZRM.

Table 1 – Impact of intracerebroventricular myriocin treatment on physiological parameters in obese Zucker rats.

	LZR	LZRM	OZR	OZRM
Weight (g)	347 ± 12	353 ± 4	494 ± 22**$$$**	470 ± 1 **&&&**
Cumulative food intake (g/kg)	1774.93 ± 37.22	1800.45 ± 34.27	1738.40 ± 73.59	1652.30 ± 47.45
% Fat	8.7 ± 0.75	8.7 ± 0.16	42.9 ± 1.7 **$$$**	41.9 ± 1.5 **&&&**
% Lean	76 ± 0.9	75 ± 1.1	46 ± 1.5 **$$$**	47 ± 1.3 **&&&**
Glucose (mg/dl)	101 ± 3.1	107 ± 7.3	133 ± 2.7 **$$$**	117 ± 5.4*
Insulin (ng/ml)	0.27 ± 0.04	0.18 ± 0.07	3.58 ± 1.75 **$$$**	5.88 ± 2.2* **&&&**
FFA (mmol/l)	0.56 ± 0.03	0.55 ± 0.12	2.24 ± 0.18 **$$**	1.44 ± 0.18*
TG (mg/dl)	79.6 ± 16.3	116.7 ± 32.3	794.3 ± 126.1 **$$$**	259.2 ± 29***
Glycerol (mmol/l)	1.10 ± 0.09 **&**	1.56 ± 0.15	0.910 ± 0.157	3,077 ± 0.43***
SAFA (μg/ml)	697.91 ± 35.82	690.21 ± 12.28	2342.88 ± 108.47 **$$$**	1735.57 ± 144.61**
MUFA (μg/ml)	1516.33 ± 299.21	1566.51 ± 184.11	5719.63 ± 884.06 **$$**	3618.79 ± 719.14*
PUFA (μg/ml)	13.99 ± 2.78	12.28 ± 5.24	375.75 ± 27.25 **$**	151.68 ± 43.26
Ceramide (pmol/nmol of PL)	8.03 ± 2.04	7.34 ± 2.15	17.38 ± 4.02 **$**	19.01 ± 4.73#

Lean and obese Zucker rats were injected intracerebroventricularly with a mini pump with 300 nM of myriocin (LZRM, OZRM) or saline (LZR, OZR) during 28 days. Weight, cumulative food intake, % fat and % lean were measured at the end of treatment. Prior to sacrifice, animals were fasted during 18 h and plasmatic parameters were measured: triglycerides, free fatty acids, glycerol, SAFA, MUFA, PUFA and ceramide levels. FFA: Free fatty acids, TG: Triglyceride, SAFA: Saturated Fatty Acids; MUFA: Monounsaturated Fatty Acids; PUFA: polyunsaturated Fatty Acids. n = 6–8 animals per experimental group. *p < 0.05; ***p < 0.001 OZR vs OZRM; &p < 0.05; &&p < 0.01 LZR vs LZRM; &&&p < 0.001 LZRM vs OZRM; $$$p < 0.001 LZR vs OZR; #p < 0.05 LZR vs OZRM.

 © 2017 The Authors. Published by Elsevier GmbH. This is an open access article under the CC BY-NC-ND license (http://creativecommons.org/licenses/by-nc-nd/4.0/).

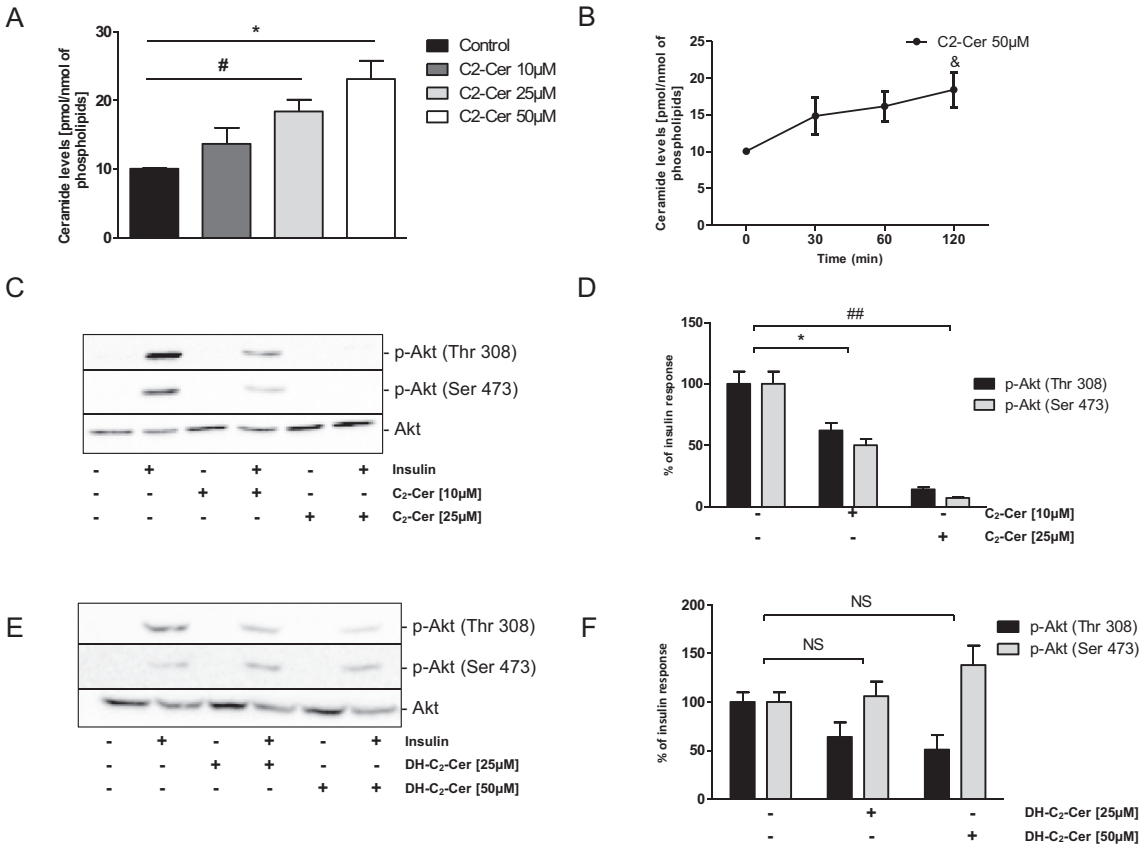

Figure 2: Effect of hypothalamic exogenous ceramide metabolism on insulin resistance in GT1-7 cells. (A) GT1-7 cells were treated with different concentrations of C_2-Ceramide for 2 h. Cells lysate were used to determine intracellular ceramide content by the DAG kinase method. (B) Conversion of 50 μM of C_2-Ceramides to endogenous ceramides. n = 3. Error bars represent SEM; *p < 0.05 control versus C_2-Ceramide 25 μM, #p < 0.05 control versus C_2-Ceramide 50 μM, &p < 0.05 Time 0 vs Time 120. (C-D-E-F) GT1-7 cells were treated with different concentrations of C_2-Ceramide (10 μM and 25 μM) or DH-C_2-Ceramides (25 μM and 50 μM) for 2 h and then with insulin (100 nM) during 5 min prior to cell lysis and immunoblotting. (C-E) Akt phosphorylation was determined in cell lysates. (D—F) Quantification of WB expressed as % of insulin response. Immunoblots are representative of three separate experiments. Error bars represent SEM; *p < 0.05 control versus C2-Ceramide 10 μM, ##p < 0.01 control versus C2-Ceramide 25 μM.

3.3. Palmitate induced *de novo* ceramide synthesis in hypothalamic GT1-7 cells

Saturated fatty acids, and especially palmitate, are drastically increased in plasma of OZR (Table 1 and Figure S2B), suggesting that these fatty acids could cross the blood brain barrier and induce hypothalamic lipotoxicity. Interestingly, we found that palmitate accumulated in hypothalamic GT1-7 cells after 24 h of treatment (Figure 3A) and increased ceramide levels by almost two-fold (Figure 3D) without affecting the mRNA levels of enzymes involved in *de novo* ceramide synthesis (Figure 3C). Myriocin significantly reduced palmitate-induced ceramide accumulation in GT1-7 cells (Figure 3D). When GT1-7 cells were incubated with deuterated palmitate (d4-palmitate) and analyzed by LC-MS/MS, we found that palmitate can be incorporated into the sphingoid base backbone (will form d4-ceramides), acyl chain (will form d4-ceramides), or both to generate d8-ceramide species (Figure 3B). The d4-palmitate labelling increased both d4-ceramide and d8-ceramide in GT1-7 cells (Figure 3D,E) including C16:0, C18:0, C22:0, and C24:0 species (Figure 3F,G and H). Looking at ceramide species, d4-palmitate incorporated in both chain of C16:0 and C18:0 ceramide forming d8-ceramide species whereas C22:0 and C24:0 ceramide species exist only as d4-ceramide forms. Analysis of mono-labeled d4-C16:0 and C18:0 ceramides revealed a major labeling in the N-acyl chain (Figure S1F), reflecting that they are synthesized from existing DHSph or sphingosine via ceramide synthases (CerS). In contrast, C22:0 ceramide incorporated d4-palmitate either in the sphingoid backbone or the N-acyl chain, whereas C24:0 ceramide was mostly labeled in the sphingoid backbone (Figure S1F), supporting a direct role of SPT activity in their synthesis. As expected, base labeling was totally inhibited by myriocin since only d4-ceramides were observed (Figure 3I,J, and K) which originated from N-acyl chain labeling. Interestingly, accumulation of C22:0 and C24:0 d4-ceramides was totally blocked by myriocin (Figure 3L), while incorporation of d4-palmitate into C16:0 and C18:0 ceramides was not affected. These findings suggest that palmitate-induced accumulation of selective ceramide species is dependent on either SPT or CerS activity in hypothalamic GT1-7 cells.

3.4. Palmitate induces insulin resistance through the *de novo* ceramide synthesis in GT1-7 cells

Palmitate treatment induced insulin resistance by decreasing Akt phosphorylation (Figure 4A,B). Addition of myriocin counteracted the effects of palmitate by restoring insulin-induced Akt phosphorylation (Figure 4A,B). Identical results were obtained with another potent inhibitor of SPT, L-cycloserine, (Figure S1C, D and E). To definitively

 © 2017 The Authors. Published by Elsevier GmbH. This is an open access article under the CC BY-NC-ND license (http://creativecommons.org/licenses/by-nc-nd/4.0/).

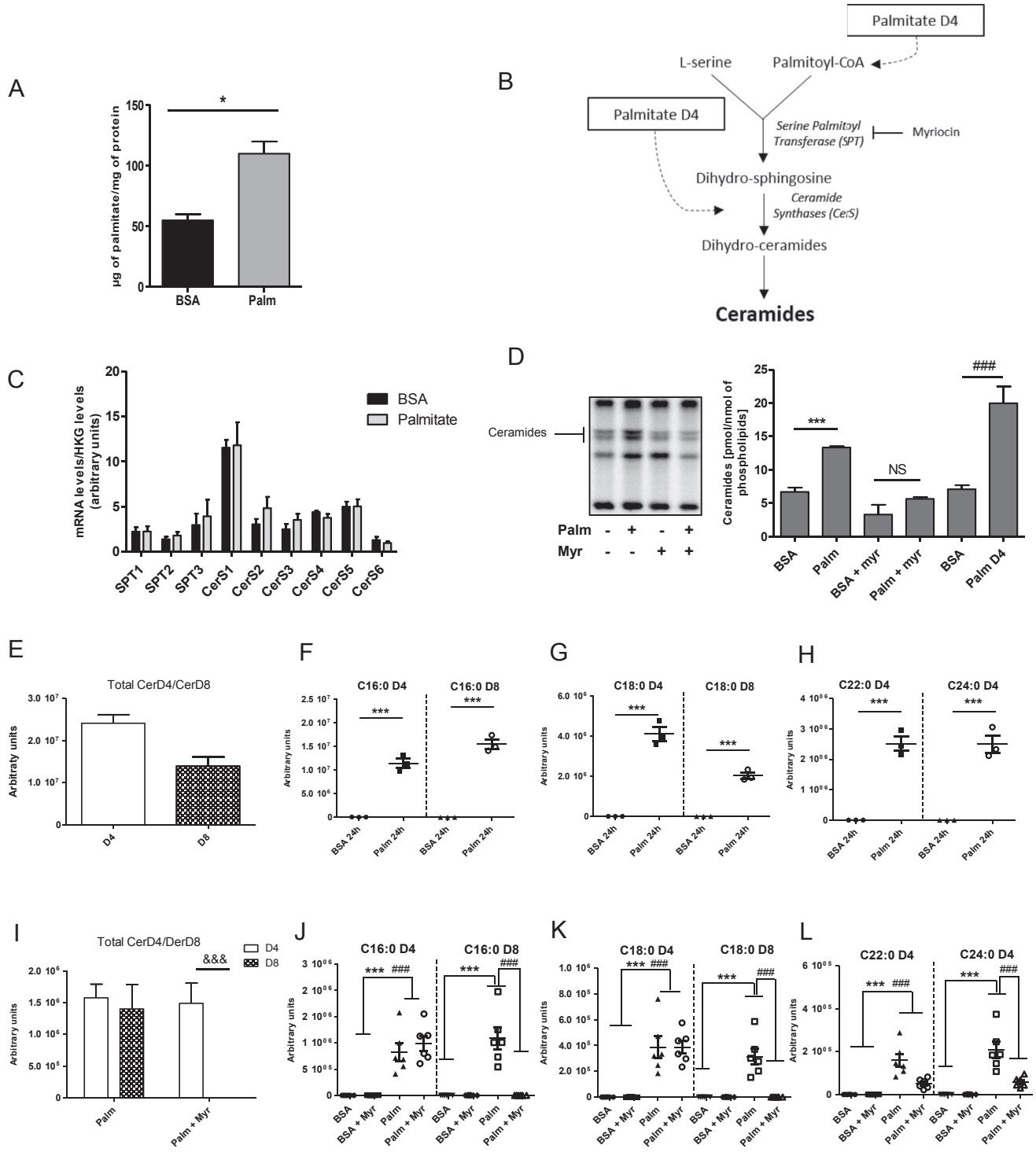

Figure 3: Effect of palmitate on ceramide production in GT1-7 cells. (A—C) GT1-7 cells were incubated with 1 mM of palmitate or BSA as a control for 24 h. (A) Amount of palmitate on GT1-7 cells after incubation, n = 3 per experimental group. Error bars represent SEM; *p < 0.05 BSA vs Palmitate. (C) mRNA levels were determined. (B) Representative scheme of the *de novo* synthesis pathway. (D-E-F-G-H-I-J-K-L) GT1-7 cells were incubated with 1 mM of palmitate, d4-palmitate or BSA as a control for 24 h with or without 10 µM of myriocin. Total ceramide levels were determined in cell lysate by the DAG kinase method (D) or by lipidomic analysis (E—L). Total amount of Cer-D4 and Cer-D8 (D) and ceramide species in GT1-7 treated with Palmitate D4 (F-G-H). Total amount of Cer-D4 and -D8 (I) and (J-K-L) in GT1-7 treated with d4-palmitate with or without 10 µM of myriocin n = 3 per experimental group, Error bars represent SEM; ***p < 0.001 BSA vs Palmitate D4; ###p < 0.001 BSA + Myr vs Palmitate D4 + Myr; &&&p < 0.001 Palm D4 + Myr vs Palm D4 + Myr.

 © 2017 The Authors. Published by Elsevier GmbH. This is an open access article under the CC BY-NC-ND license (http://creativecommons.org/licenses/by-nc-nd/4.0/).

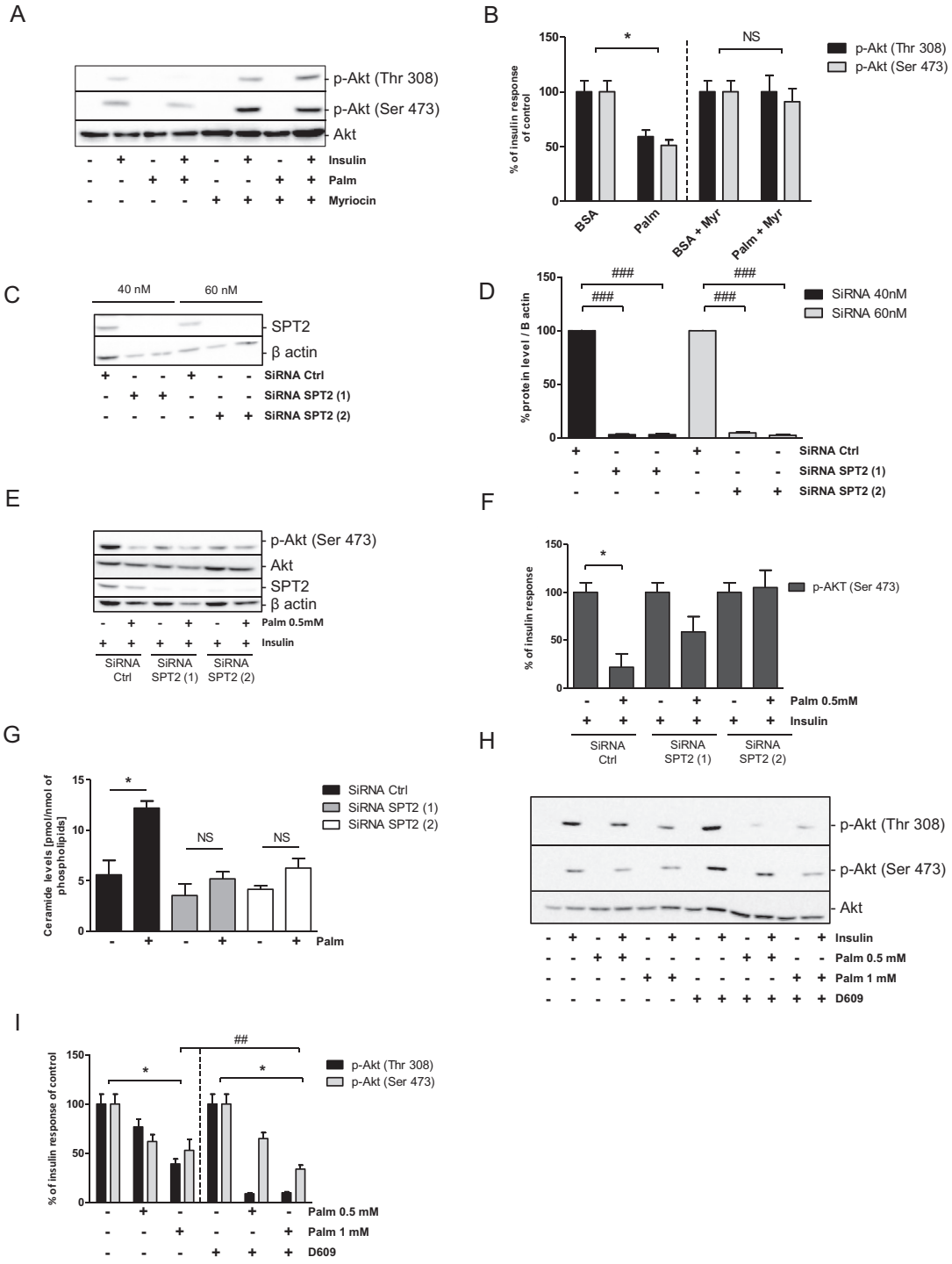

Figure 4: Involvement of *de novo* synthesis pathways on palmitate-induced insulin resistance in GT1-7 cells. (A) GT1-7 cells were incubated with 1 mM of palmitate or BSA as a control for 24 h. PhosphoAkt was determined in cell lysates. (B) Quantification of WB expressed as % of insulin response. n = 3 per experimental group. Error bars represent SEM; *p < 0.05 BSA vs Palmitate. GT1-7 cells were incubated with 40 or 60 nM of 2 different SiRNA against SPT2. (C–D) Cell lysates were immunoblotted with specific antibodies against SPT2 or against native β-actin. (D) Quantification of WB. ###p < 0.001 SiRNA Ctrl versus SiRNA SPT2. n = 3 per experimental group. Error bars represent SEM. (E-F-G) GT1-7 cells were incubated with 40 or 60 nM of 2 different SiRNA against SPT2, then they were stimulated with 0.5 mM of palmitate or BSA for 24 h prior to incubation with 100 nM insulin for 5 min. PhosphoAkt, SPT2 levels, and β-actin (E, F), ceramide levels (G) were determined in cell lysate as described in Materials and Methods. (F) Quantification of WB expressed as % of insulin response. n = 3 per experimental group. Error bars represent SEM; *p < 0.05 BSA vs Palmitate; #p < 0.05. n = 3 per experimental group. Error bars represent SEM. (H–I) GT1-7 cells were incubated with 1 mM of palmitate or BSA as a control for 24 h with or without 10 μM of D609 prior to incubation with 100 nM insulin for 5 min. PhosphoAkt was determined in cell lysates. n = 3 per experimental group. Error bars represent SEM; *p < 0.05 BSA vs Palmitate, ##p < 0.01 Palmitate (p-Akt Thr308) vs Palmitate D609 (p-Akt Thr308), *p < 0.01 BSA D609 vs Palm D609.

 © 2017 The Authors. Published by Elsevier GmbH. This is an open access article under the CC BY-NC-ND license (http://creativecommons.org/licenses/by-nc-nd/4.0/).

confirm the involvement of *de novo* ceramide synthesis in this mechanism, we inhibited expression of SPT2 isoform using specific siRNA in GT1-7 cells. siSPT2 decreased SPT2 mRNA levels by almost three-fold (Figure S1B) resulting in a 95% reduction in SPT2 protein levels (Figure 4C,D). siSPT2 treatment did not alter basal and insulin-mediated Akt phosphorylation by itself (Figure S1C). We found that phosphorylation of Akt was restored in GT1-7 cells treated with palmitate in response to insulin when SPT2 was down-regulated (Figure 4E,F). Importantly, SPT2 down-regulation blocked ceramide accumulation induced by palmitate in GT1-7 cells (Figure 4G). Finally, we used D609, an inhibitor of sphingomyelin synthase, to block conversion of ceramide into sphingomyelin. D609 potentiates the inhibition of Akt phosphorylation induced by palmitate treatment (Figure 4H,I). Moreover, a potent inhibitor of glucosyl-ceramide synthase, N-butyldeoxynojirimycin, was also unable to alter palmitate-induced insulin resistance in GT1-7 cells (Figure S1D). Our results showed that *de novo* ceramide synthesis played a key role in IR induced by the palmitate. Moreover, it appeared that ceramide, rather than one of its metabolites, inhibited insulin-induced Akt phopshorylation in hypothalamic GT1-7 cells.

3.5. Ceramides inhibit insulin signaling through PKCζ activation in hypothalamic GT1-7 cells

In peripheral tissues, ceramides have been demonstrated to exert their toxic effects through PKCζ activation [27–29]. We found that the potent inhibitor of all PKCs, Ro31-8220 [30], counteracted the inhibition of Akt phosphorylation induced by either C_2-cer (Figure 5A,B) or palmitate (Figure 5C,D) in GT1-7 cells. Ro31-8220 did not affect palmitate-induced ceramide accumulation (Figure 5E). Interestingly, a constitutive active form of PKCζ (PKCζ-CA) mimicked the inhibitory effect of both palmitate and ceramide on insulin-induced Akt phosphorylation (Figure 5G,H). Moreover, a dominant negative form of PKCζ (PKCζ-DN) restored Akt phosphorylation in response to insulin when GT1-7 cells were treated with palmitate (Figure 5G,H, I, and J) or C_2-cer (Figure 5I,J). We found that PKCζ-DN did not affect ceramide accumulation induced by palmitate or C_2-cer treatment (Figure 5F), lending credence to the idea that PKCζ acts down-stream of ceramide synthesis. The results showed that ceramides mediate IR through PKCζ activation in hypothalamic GT1-7 cells.

3.6. Inhibition of hypothalamic ceramides improved glucose tolerance and insulin secretion in OZR

We found that central myriocin slightly improved insulin resistance in OZR without any effect in LZR (Figure 6A,B). In addition, an oral glucose tolerance test (OGTT) showed that myriocin ameliorated glucose intolerance in OZR (Figure 6C,D), suggesting a better regulation of glucose homeostasis. OZR presents already increased basal insulin levels (Figure 6E,F) reflecting their insulin resistant state. Myriocin treatment was unable to decrease basal insulin levels in OZR (Figure 6E). However, we found that improved glucose tolerance of myriocin-treated OZR is associated with a greater increase of insulin secretion in response to glucose in OZR (Figure 6E,F). Glucose regulates insulin secretion partly through its action on parasympathetic nervous system [31], [32]. Basal parasympathetic activity was increased in OZR compared to LZR (Figure 6G,H). Glucose stimulates nervous activity in LZR but not in OZR, reflecting an impaired hypothalamic regulation by glucose sensing (Figure 6G). Interestingly, myriocin treatment restored activation of parasympathetic activity by glucose in OZR (Figure 6G,H). These results suggest that hypothalamic ceramides inhibit insulin secretion by regulating parasympathetic tone in OZR.

3.7. Hypothalamic ceramides regulate insulin secretion and β-cell area in OZR

We assessed the capacity of isolated islets of Langerhans to secrete insulin in response to glucose in order to gain more insights on the up-regulation of insulin secretion when hypothalamic ceramides synthesis is inhibited, (Figure 7A). Islets from OZR were unable to secrete insulin in response to glucose compared to LZR (Figure 7A). Importantly, myriocin treatment restored the capacity of glucose-induced insulin release from OZR islets (Figure 7A). We also found that myriocin-treated OZR islets had a higher insulin content (Figure 7B). Interestingly, myriocin treatment further increased the percentage of β-cell area in OZR (Figure 7C,D, and E) without any effect in LZR (Figure S2A). The increase in β-cell area from myriocin-treated OZR is associated with the high number of small new islets (Figure 7D,E). These data suggest that hypothalamic ceramides are not only potent regulators of insulin secretion but also of β-cell area in OZR.

4. DISCUSSION

Our study showed that *de novo* ceramide synthesis in hypothalamus of OZR and in neuronal hypothalamic cells induced central IR. This implies activation of PKCζ to relay deleterious effects of ceramides. Inhibition of hypothalamic *de novo* ceramide synthesis in OZR slightly restored peripheral insulin sensitivity and drastically increased insulin-secretion and pancreatic β-cell area, which contributed to ameliorating glucose tolerance in these rats. Interestingly, inhibition of hypothalamic ceramide synthesis also improved glucose-stimulated parasympathetic nerve activity in OZR. These results suggest a new role of hypothalamic ceramides in the deregulation of central insulin signalling and glucose homeostasis induced by obesity.

Our observations that the accumulation of ceramide levels in hypothalamus of OZR and also in palmitate-treated hypothalamic cells were not associated with variation in expression of enzymes regulating *de novo* ceramide synthesis suggest that this increase is linked to modulation of enzyme activity rather than enzyme expression. This observation is in agreement with the Km (0.2 mM) of SPT, the rate limiting enzyme of *de novo* ceramide synthesis [33], which allows it to change in response to substrate variation [34]. We also found that d4-palmitate increased both mono-labeled d4-ceramides and doubled-labeled d8-ceramides in hypothalamic cells. These data suggest that palmitate required SPT activity (labelling of the sphingoid base) and also CerS activity (labeling of the N-acyl chain) to increase ceramide levels in hypothalamic cells. In agreement, myriocin only inhibited incorporation of d4-palmitate into the sphingoid base moiety of ceramide species. Interestingly, myriocin-treated OZR showed reduced ceramide accumulation in the hypothalamus, highlighting the *in vivo* role of *de novo* ceramide generation in the hypothalamus during obesity.

Ceramide metabolism has been linked to the installation of peripheral IR [12]. Central infusion of ceramide analogs induced hypothalamic IR in Wistar rats while myriocin restored insulin sensitivity in palmitate-treated hypothalamic cells and also in the hypothalamus of OZR. The absence of effect of potent inhibitors of ceramide metabolic enzymes (sphingomyelin and glucosylceramide synthase) on palmitate-induced insulin resistance strongly suggests that ceramides are the mediators of insulin resistance in hypothalamic cells. Interestingly, in hypothalamic cells, myriocin treatment associated with d4-labeled palmitate specifically decreased C22:0 and C24:0 ceramide species, suggesting a key role of the *de novo* synthesis of very long chain ceramides in IR installation. Interestingly, Elovl1 which catalyzes the production of C24:0 FFAs has been linked to C24 ceramide synthesis through its

 © 2017 The Authors. Published by Elsevier GmbH. This is an open access article under the CC BY-NC-ND license (http://creativecommons.org/licenses/by-nc-nd/4.0/).

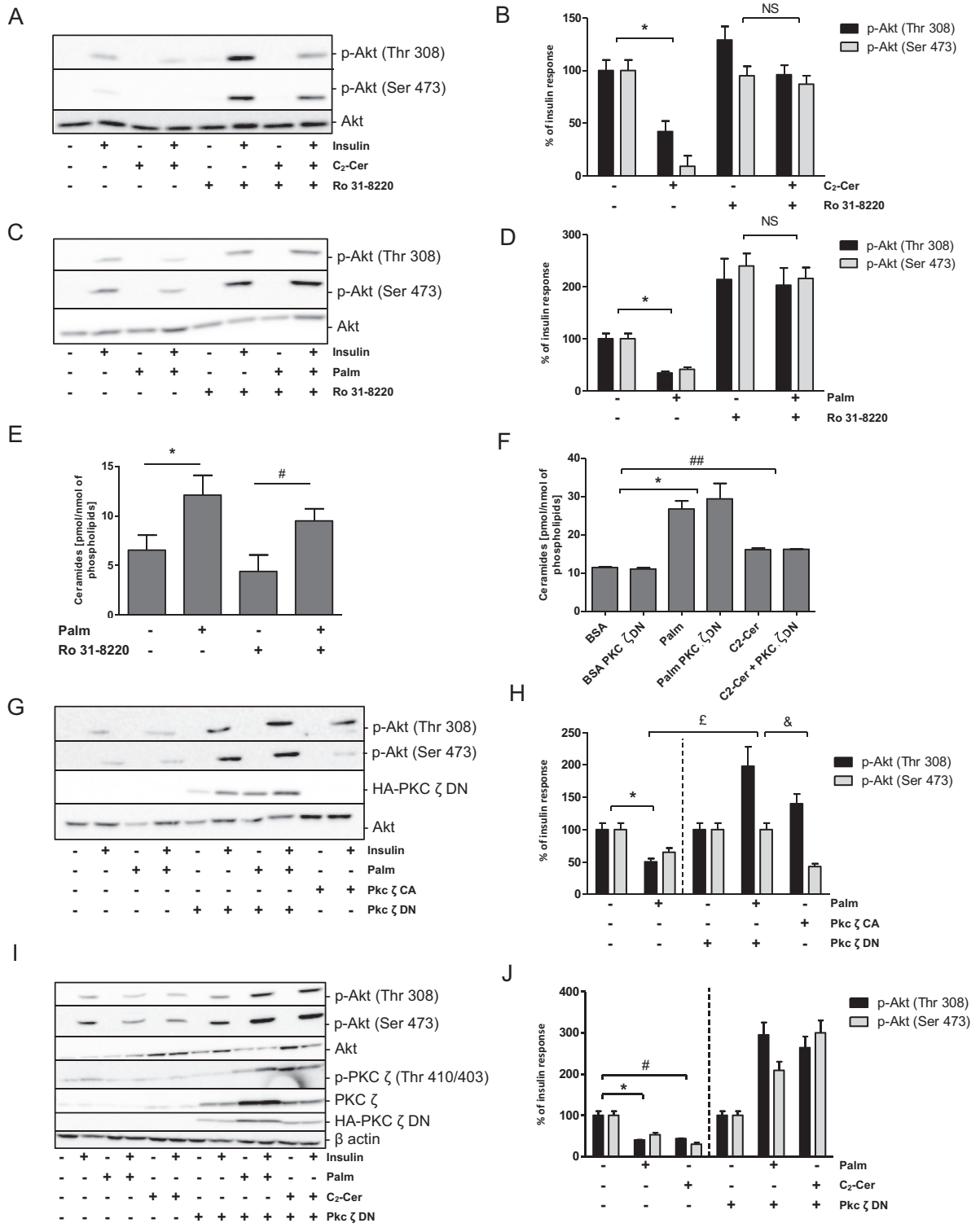

Figure 5: Role of PKCζ in insulin-resistance induced by palmitate and exogenous ceramides in GT1-7 cells. (A-B-C-D-E) Cells were treated with 25 μM of C_2-Ceramide for 2 h or with 1 mM of palmitate or BSA as a control for 24 h with or without 5 μM of Ro 31-8220 prior to incubation with 100 nM insulin for 5 min (A-B-C-D) Phospho-Akt and (E) ceramide levels were determined in cell lysates. (B-D) Quantification of WB expressed as % of insulin response n = 3 per experimental group. Error bars represent SEM; *p < 0.05 BSA vs Palmitate, #p < 0.05 BSA + Ro 31-8220 vs Palmitate + Ro 31-8220. (F-G-H-I-J) GFP, PKC ζ DN or PKC ζ CA-GT1-7 infected cells were treated with 1 mM of palmitate for 24 h (G—H) or with 25 μM of C_2-Ceramide for 2 h (I—J) prior to incubation with 100 nM insulin for 5 min (G-H-I-J) Phospho-Akt, p-PKC ζ (Thr410/403), native PKC ζ, HA-PKC ζ-DN or β actin levels and (F) ceramide levels were determined in cell lysates. (H—J) Quantification of WB expressed as % of insulin response. n = 3 per experimental group. Error bars represent SEM; *p < 0.05, BSA vs Palmitate, £p < 0.05 Palmitate vs Palmitate + PKC ζ DN, &p < 0.05 Palmitate PKC ζ DN vs PKC ζ CA, #p < 0.05, ##p < 0.01 BSA vs C_2-Cer.

 © 2017 The Authors. Published by Elsevier GmbH. This is an open access article under the CC BY-NC-ND license (http://creativecommons.org/licenses/by-nc-nd/4.0/).

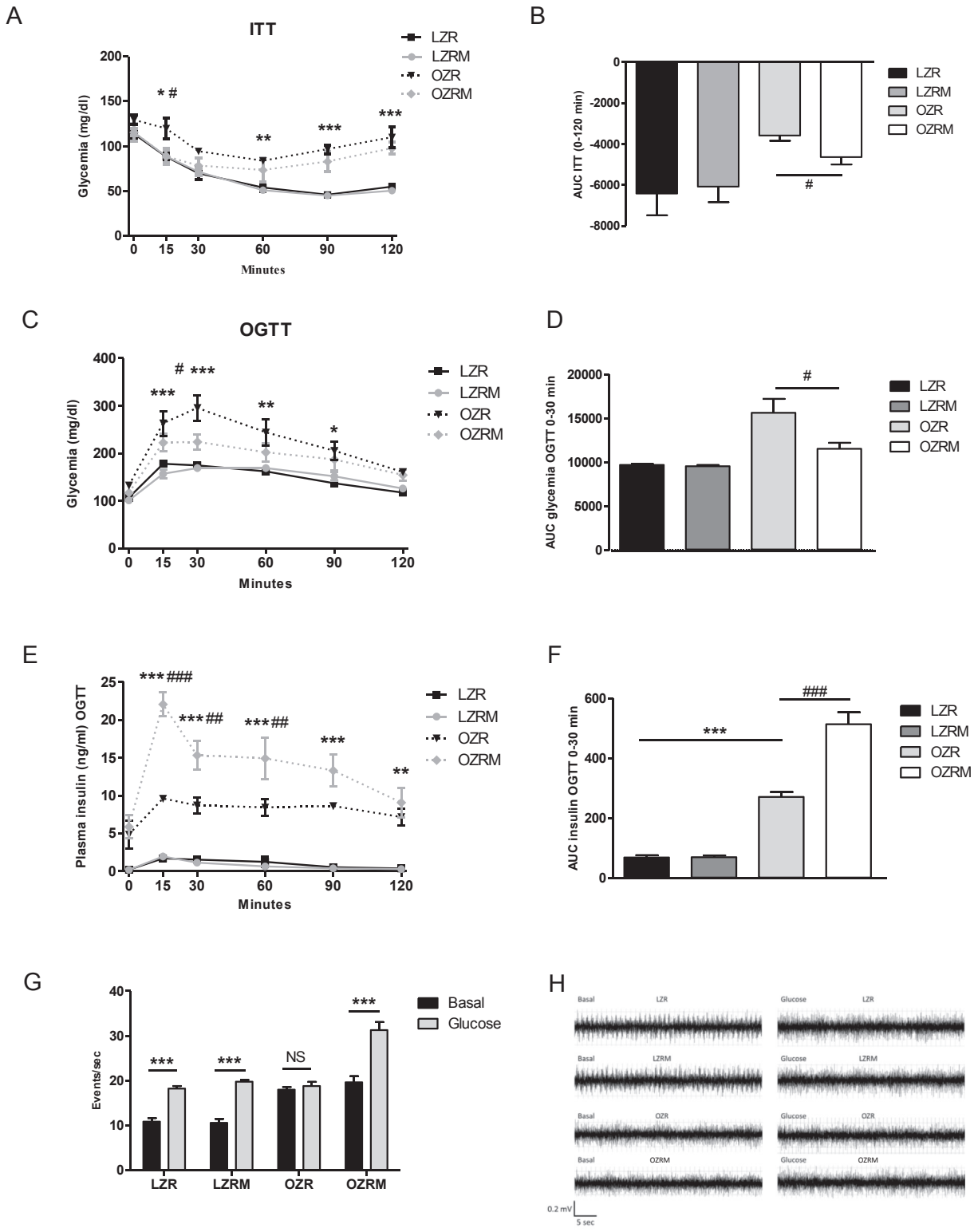

Figure 6: Effect of hypothalamic ceramides on glucose homeostasis in obese Zucker rats. (A-B-C-D-E-F-G) Zucker lean and obese rats were ICV injected using a mini-pump containing 300 nM of myriocin (LZRM, OZRM) or NaCl 9‰ (LZR, OZR) during 28 days. (A—B) An insulin tolerance test (ITT) was performed. (A) Blood glucose, (B) area under the curve of blood glucose. (C-D-E-F) An oral glucose tolerance test (OGTT) was performed. (C) Blood glucose, (D) area under the curve of blood glucose, (E) plasma insulin levels, (F) area under the curve of plasma insulin levels. Error bars represent SEM; n = 6—8 animals per experimental group. *p < 0.05, **p < 0.01, ***p < 0.001 LZR vs OZR, #p < 0.05, ##p < 0.01, ###p < 0.001 OZR vs OZRM. (G—H) 30min, prior to sacrifice, nervous parasympathetic activity was recorded during 15 min to have basal values. Then, animals received an intraperitoneal injection of glucose (3 g/kg) to stimulate the parasympathetic nervous system and this nervous activity was recorded during 15 min. Results are expressed on events/sec. Error bars represent SEM; n = 6—8 animals per experimental group. **p < 0.01 basal vs glucose.

 © 2017 The Authors. Published by Elsevier GmbH. This is an open access article under the CC BY-NC-ND license (http://creativecommons.org/licenses/by-nc-nd/4.0/).

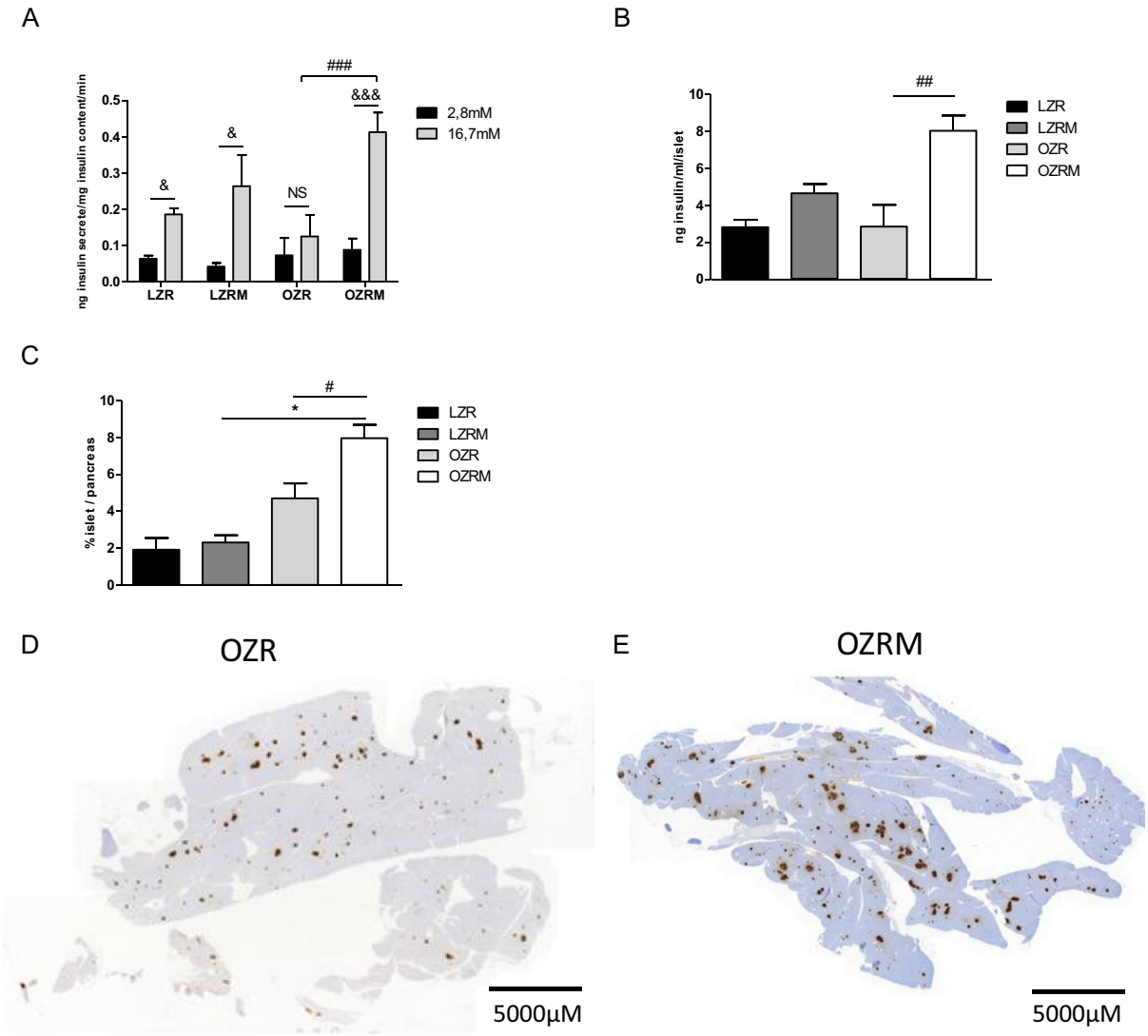

Figure 7: Effect of hypothalamic ceramides on β-cell function and area in obese Zucker rats. (A-B-C-D) Zucker lean and obese rats were ICV injected using mini-pump containing 300 nM of myriocin (LZRM, OZRM) or NaCl 9‰ (LZR, OZR) during 28 days. Prior to sacrifice, animals were fasted during 18 h. (A-B-C-D) Pancreata were taken and were used for *ex vivo* experiments and to quantified β-cell area. Islets of Langerhans were isolated; then they were stimulated with low (2.8 mM) of high (16.7 mM) glucose concentration during 90 min and supernatant were taken. Islets were lysates to measure the insulin content. An ELISA test was performed to measure insulin. (A) glucose-stimulated insulin secretion by isolated islets of Langerhans, (B) insulin content of islets, (C) percentage of β-cell area, (D) Immunodetection of insulin (brown) in pancreatic sections of OZR with or without myriocin. Hematoxylin staining was used to counterstain the tissue. Error bars represent SEM; n = 6–8 animals per experimental group. *p < 0.001 LZR vs OZR, ##p < 0.01, ###p < 0.001 OZR vs OZRM, &p < 0.01, &&&p < 0.001 2.8 vs 16.7 mM of glucose.

interaction with CerS2 [35]. Therefore, future experiments will be required to determine the precise role of Elovl1 and CerS2 in ceramide-induced hypothalamic IR. In addition, we and others have shown that ceramide analogs were recycled into long chain ceramide in hypothalamus [10], which involved ceramide synthase activities [36]. Therefore, this approach will also be interesting to explore the role of ceramide synthase isoforms in hypothalamic insulin resistance. Ceramides are potent activators of PKCζ [37], a highly expressed kinase in a few areas in the rat brain including the hypothalamus [38] and, specifically, the arcuate and paraventricular nuclei, both key sites of insulin action [39]. A dominant negative form of PKCζ totally prevented hypothalamic IR induced by ceramide. To our knowledge, this is the first demonstration of a link between ceramides, PKCζ activation, and IR in hypothalamic cells. Amplification of monocyte/macrophage innate immune responses required metabolism of ceramide and activation of PKCζ/mitogen-activated protein kinases [40]. Thus activation of PKCζ by ceramides in central nervous system (CNS) would probably induce more than IR, and could also lead to neurodegeneration [41]. Moreover, the use of GT1-7 cells, which originated from GnRH neuronal cells [15] could imply dysregulation of hypothalamic-pituitary-gonadal axis by ceramides and therefore fertility's problems [42]. Interestingly, PKCζ has been already involved in peripheral insulin resistance [12] suggesting that a unique role of this PKC isoform in the regulation of insulin sensitivity by ceramides. However, peripheral insulin resistance has also been associated with various signaling pathways such as PP2A or double-stranded RNA-dependent protein kinase [12]. Therefore, it will be important to explore in the future the potential link that could be exist between these pathways and the ceramide-induced hypothalamic insulin resistance.

 © 2017 The Authors. Published by Elsevier GmbH. This is an open access article under the CC BY-NC-ND license (http://creativecommons.org/licenses/by-nc-nd/4.0/).

Infusion of ceramide analogs in the hypothalamus have been shown to induce weight gain through up-regulation of ER stress [10]. Interestingly, it has been shown that inhibition of ER stress in response to increased ceramide levels in the hypothalamus of OZR, improved energy balance without affecting food intake [10]. We found that infusion of myriocin did not induce weight changes in OZR even if hypothalamic insulin signaling was restored, suggesting that endogenous hypothalamic ceramides seemed to not regulate feeding behavior in OZR. However, the increased feeding of OZR due to leptin resistance [25] could mask the effect of hypothalamic ceramide on regulation of food intake by insulin. In contrast, we found that hypothalamic *de novo* ceramide synthesis is a critical regulator of glucose homeostasis in OZR. This was supported by our observations that myriocin partially restored glucose tolerance in OZR. Inhibition of hypothalamic ER stress did not alter glucose intolerance in OZR [15], suggesting that hypothalamic ceramides could regulate glucose homeostasis independently of ER stress. However, we cannot exclude that a more prolonged inhibition of hypothalamic ER stress, as we did for ceramide synthesis, could be required to regulate glucose homeostasis. We found that inhibition of *de novo* ceramide synthesis, as with inhibition of ER stress in hypothalamus of OZR, was associated with a slight effect on peripheral insulin sensitivity. In contrast, improved glucose tolerance in myriocin-treated OZR was associated with a significant increase in insulin secretion and also pancreatic β-cell area, a phenomenon which is not observed when ER stress is inhibited in OZR [10] suggesting different molecular mechanisms. Interestingly, glucose-induced insulin secretion was restored in islets of myriocin-treated OZR. It has been shown that dysfunction of hypothalamic insulin receptors results in islet dysfunction (56). Therefore, a potential link between hypothalamic IR in OZR and a defect of insulin secretion regulated by ceramide remains to be determined. Altogether, our results suggest that hypothalamic ceramides modulate pancreatic β-cell function and area to alter glucose homeostasis in obese rats.

Pancreatic islet function is known to be controlled by CNS [43], such as parasympathetic system which is a key regulator of islet function and insulin release [44,45]. It is also known that glucose stimulates parasympathetic activity in order to stimulate insulin secretion [46]. Interestingly, we found that myriocin-treated OZR showed a restored glucose-stimulating vagal activity, reflecting parasympathetic tonus, suggesting that this mechanism could be involved in increased insulin secretion in these rats. The identity of neurons regulating insulin secretion in response to glucose remains unknown. POMC neurons in the arcuate nucleus have been shown to be glucose excited [47] and found to regulate parasympathetic activity [48]. Loss of mitochondrial flexibility in POMC neurons altered glucose sensing, resulting in defective insulin secretion [49]. Interestingly, ceramide metabolism has been linked to the regulation of mitochondria dynamics [50]. Therefore, hypothalamic ceramide could inhibit glucose sensing in POMC neurons by affecting mitochondrial function, which will block insulin secretion regulated by parasympathetic tone. A role of the parasympathetic system in the control of the β-cell mass has also been described. Lesions of the ventromedial hypothalamus increased β-cell proliferation through parasympathetic hyperactivity [43]. In addition, Thorens and co-workers showed that the glucose transporter 2 controls glucose-activating parasympathetic tonus, which stimulates β-cell proliferation [31]. These studies suggest that hypothalamic ceramides could regulate insulin secretion and also β-cell area by inhibiting parasympathetic activity.

In conclusion, our study revealed that *de novo* ceramide synthesis plays a key role in the installation of hypothalamic insulin resistance and contributed to the deregulation of glucose homeostasis induced by obesity. In particular, hypothalamic ceramides appear to be critical regulators of insulin secretion and β-cell area regulated by the parasympathetic nervous system. This could provide the future basis of novel pharmaceutical interventions for the treatment of obesity and its complications.

CONFLICT OF INTEREST

All authors declare that they have no conflict of interest.

AUTHOR CONTRIBUTIONS

HLS, CR, MC, and CM contributed to the study concept and design, analysis and interpretation of the data. MC, LB, CR, LR, NC, CLB, EP, KM, NK, JD, and CM contributed to the acquisition of the data. EH and CLB contributed reagents/materials/analytical tools. NB and BC performed the lipidomic analysis. HLS, MC, and CM wrote/edited the manuscript with contributions from EH and LR. HLS is responsible for its content. All authors revised the article and approved the final version. The authors thank Carl Ng, School of Biology and Environmental Science, University College Dublin, Belfield, Ireland, for help with preparing the manuscript.

ACKNOWLEDGMENT

This project was supported by grants from Centre National de la Recherche Scientifique (CNRS), the Innovative Medicines Initiative Joint Undertaking under grant agreement no 155005 (IMIDIA) and the Agence Nationale de la Recherche (ANR PRCI-15-CE14-0027-01 BetaDiamark). M. Campana received a doctoral fellowship from the CORDDIM, Ile-de-France. L. Bellini received a doctoral fellowship supported by IMIDIA-ENSO (IMIDIA: 155005). N. Coant received a post-doctoral fellowship from the French Society of Nutrition (SFN). This work was also supported by MetaboHUB (ANR-11-INBS-0010). All authors declare that they have no conflict of interest.

APPENDIX A. SUPPLEMENTARY DATA

Supplementary data related to this article can be found at https://doi.org/10.1016/j.molmet.2017.10.013

REFERENCES

[1] González-García, I., Fernø, J., Diéguez, C., Nogueiras, R., López, M., 2017. Hypothalamic lipids: key regulators of whole body energy balance. Neuroendocrinology 104(4):398—411.

[2] Magnan, C., Levin, B.E., Luquet, S., 2015 Dec. Brain lipid sensing and the neural control of energy balance. Molecular and Cellular Endocrinology 418:3—8.

[3] Le Stunff, H., Coant, N., Migrenne, S., Magnan, C., 2013 Jun. Targeting lipid sensing in the central nervous system: new therapy against the development of obesity and type 2 diabetes. Expert Opinion on Therapeutic Targets 17(5): 545—555.

[4] Benoit, S.C., Kemp, C.J., Elias, C.F., Abplanalp, W., Herman, J.P., Migrenne, S., et al., 2009 Sep 1. Palmitic acid mediates hypothalamic insulin resistance by altering PKC-θ subcellular localization in rodents. Journal of Clinical Investigation 119(9):2577—2589.

[5] Cruciani-Guglielmacci, C., Hervalet, A., Douared, L., Sanders, N.M., Levin, B.E., Ktorza, A., et al., 2004 Nov. Beta oxidation in the brain is required for the effects of non-esterified fatty acids on glucose-induced insulin secretion in rats. Diabetologia 47(11):2032—2038.

 © 2017 The Authors. Published by Elsevier GmbH. This is an open access article under the CC BY-NC-ND license (http://creativecommons.org/licenses/by-nc-nd/4.0/).

[6] Obici, S., Feng, Z., Arduini, A., Conti, R., Rossetti, L., 2003 Jun. Inhibition of hypothalamic carnitine palmitoyltransferase-1 decreases food intake and glucose production. Nature Medicine 9(6):756–761.

[7] Alam, N., Saggerson, E.D., 1998 Aug 15. Malonyl-CoA and the regulation of fatty acid oxidation in soleus muscle. Biochemical Journal 334(Pt 1):233–241.

[8] Oh, H., Boghossian, S., York, D.A., Park-York, M., 2013 Nov. The effect of high fat diet and saturated fatty acids on insulin signaling in the amygdala and hypothalamus of rats. Brain Research 1537:191–200.

[9] Borg, M.L., Omran, S.F., Weir, J., Meikle, P.J., Watt, M.J., 2012 Sep. Consumption of a high-fat diet, but not regular endurance exercise training, regulates hypothalamic lipid accumulation in mice: high-fat diet regulates hypothalamic lipid accumulation. Journal of Physiology 590(17):4377–4389.

[10] Contreras, C., González-García, I., Martínez-Sánchez, N., Seoane-Collazo, P., Jacas, J., Morgan, D.A., et al., 2014 Oct. Central ceramide-induced hypothalamic lipotoxicity and er stress regulate energy balance. Cell Reports 9(1):366–377.

[11] Martínez-Sánchez, N., Seoane-Collazo, P., Contreras, C., Varela, L., Villarroya, J., Rial-Pensado, E., et al., 2017 Jul. Hypothalamic AMPK-ER stress-JNK1 Axis mediates the central actions of thyroid hormones on energy balance. Cell Metabolism 26(1), 212–229.e12.

[12] Bellini, L., Campana, M., Mahfouz, R., Carlier, A., Véret, J., Magnan, C., et al., 2015. Targeting sphingolipid metabolism in the treatment of obesity/type 2 diabetes. Expert Opinion on Therapeutic Targets 19(8):1037–1050.

[13] Chavez, J.A., Summers, S.A., 2012 May. A Ceramide-centric view of insulin resistance. Cell Metabolism 15(5):585–594.

[14] Blouin, C.M., Prado, C., Takane, K.K., Lasnier, F., Garcia-Ocana, A., Ferré, P., et al., 2010 Mar. Plasma membrane subdomain compartmentalization contributes to distinct mechanisms of ceramide action on insulin signaling. Diabetes 59(3):600–610.

[15] Mellon, P.L., Windle, J.J., Goldsmith, P.C., Padula, C.A., Roberts, J.L., Weiner, R.I., 1990 Jul. Immortalization of hypothalamic GnRH neurons by genetically targeted tumorigenesis. Neuron 5(1):1–10.

[16] Gerozissis, K., Orosco, M., Rouch, C., Nicolaidis, S., 1997 Oct. Insulin responses to a fat meal in hypothalamic microdialysates and plasma. Physiology & Behavior 62(4):767–772.

[17] Véret, J., Coant, N., Berdyshev, E.V., Skobeleva, A., Therville, N., Bailbé, D., et al., 2011 Aug 15. Ceramide synthase 4 and de novo production of ceramides with specific N-acyl chain lengths are involved in glucolipotoxicity-induced apoptosis of INS-1 β-cells. Biochemical Journal 438(1):177–189.

[18] Van Veldhoven, P.P., Mannaerts, G.P., 1987 Feb 15. Inorganic and organic phosphate measurements in the nanomolar range. Analytical Biochemistry 161(1):45–48.

[19] Picard, A., Rouch, C., Kassis, N., Moullé, V.S., Croizier, S., Denis, R.G., et al., 2014 Apr. Hippocampal lipoprotein lipase regulates energy balance in rodents. Molecular Genetics and Metabolism 3(2):167–176.

[20] Folch, J., Lees, M., Sloane Stanley, G.H., 1957 May. A simple method for the isolation and purification of total lipides from animal tissues. Journal of Biological Chemistry 226(1):497–509.

[21] Seyer, A., Boudah, S., Broudin, S., Junot, C., Colsch, B., 2016 May. Annotation of the human cerebrospinal fluid lipidome using high resolution mass spectrometry and a dedicated data processing workflow [cited 2017 Jul 18] Metabolomics [Internet] 12(5). Available from: http://link.springer.com/10.1007/s11306-016-1023-8.

[22] Rachdi, L., Kariyawasam, D., Aïello, V., Herault, Y., Janel, N., Delabar, J.-M., et al., 2014 Jul 15. Dyrk1A induces pancreatic β cell mass expansion and improves glucose tolerance. Cell Cycle 13(14):2221–2229.

[23] Rachdi, L., Marie, J.-C., Scharfmann, R., 2003 Jan. Role for VPAC2 receptor-mediated signals in pancreas development. Diabetes 52(1):85–92.

[24] Araujo, P., Nguyen, T.-T., Frøyland, L., Wang, J., Kang, J.X., 2008 Nov. Evaluation of a rapid method for the quantitative analysis of fatty acids in various matrices. Journal of Chromatography A 1212(1–2):106–113.

[25] Carvalheira, J.B.C., Ribeiro, E.B., Araujo, E.P., Guimaraes, R.B., Telles, M.M., Torsoni, M., et al., 2003 Dec 1. Selective impairment of insulin signalling in the hypothalamus of obese Zucker rats. Diabetologia 46(12):1629–1640.

[26] Bielawska, A., Crane, H.M., Liotta, D., Obeid, L.M., Hannun, Y.A., 1993 Dec 15. Selectivity of ceramide-mediated biology. Lack of activity of erythro-dihydroceramide. Journal of Biological Chemistry 268(35):26226–26232.

[27] Bourbon, N.A., Sandirasegarane, L., Kester, M., 2002 Feb 1. Ceramide-induced inhibition of Akt is mediated through protein kinase Czeta: implications for growth arrest. Journal of Biological Chemistry 277(5):3286–3292.

[28] Chavez, J.A., Knotts, T.A., Wang, L.-P., Li, G., Dobrowsky, R.T., Florant, G.L., et al., 2003 Mar 21. A role for ceramide, but not diacylglycerol, in the antagonism of insulin signal transduction by saturated fatty acids. Journal of Biological Chemistry 278(12):10297–10303.

[29] Turban, S., Hajduch, E., 2011 Jan 21. Protein kinase C isoforms: mediators of reactive lipid metabolites in the development of insulin resistance. FEBS Letters 585(2):269–274.

[30] McKenna, J.P., Hanson, P.J., 1993 Aug 17. Inhibition by Ro 31-8220 of acid secretory activity induced by carbachol indicates a stimulatory role for protein kinase C in the action of muscarinic agonists on isolated rat parietal cells. Biochemical Pharmacology 46(4):583–588.

[31] Tarussio, D., Metref, S., Seyer, P., Mounien, L., Vallois, D., Magnan, C., et al., 2014 Jan 2. Nervous glucose sensing regulates postnatal β cell proliferation and glucose homeostasis. Journal of Clinical Investigation 124(1):413–424.

[32] Colombani, A.-L., Carneiro, L., Benani, A., Galinier, A., Jaillard, T., Duparc, T., et al., 2009 Oct 1. Enhanced hypothalamic glucose sensing in obesity: alteration of redox signaling. Diabetes 58(10):2189–2197.

[33] Perry, D.K., Bielawska, A., Hannun, Y.A., 2000. Quantitative determination of ceramide using diglyceride kinase. Methods in Enzymology 312:22–31.

[34] Merrill, A.H., Wang, E., Mullins, R.E., 1988 Jan 12. Kinetics of long-chain (sphingoid) base biosynthesis in intact LM cells: effects of varying the extracellular concentrations of serine and fatty acid precursors of this pathway. Biochemistry (Mosc) 27(1):340–345.

[35] Ohno, Y., Suto, S., Yamanaka, M., Mizutani, Y., Mitsutake, S., Igarashi, Y., et al., 2010 Oct 26. ELOVL1 production of C24 acyl-CoAs is linked to C24 sphingolipid synthesis. Proceedings of the National Academy of Sciences 107(43):18439–18444.

[36] Ogretmen, B., Pettus, B.J., Rossi, M.J., Wood, R., Usta, J., Szulc, Z., et al., 2002 Apr 12. Biochemical mechanisms of the generation of endogenous long chain ceramide in response to exogenous short chain ceramide in the a549 human lung adenocarcinoma cell line: role for endogenous ceramide in mediating the action of exogenous ceramide. Journal of Biological Chemistry 277(15):12960–12969.

[37] Wang, M.Y., Koyama, K., Shimabukuro, M., Newgard, C.B., Unger, R.H., 1998 Jan 20. OB-Rb gene transfer to leptin-resistant islets reverses diabetogenic phenotype. Proceedings of the National Academy of Sciences of the United States of America 95(2):714–718.

[38] Naik, M.U., Benedikz, E., Hernandez, I., Libien, J., Hrabe, J., Valsamis, M., et al., 2000 Oct 16. Distribution of protein kinase Mzeta and the complete protein kinase C isoform family in rat brain. Journal of Comparative Neurology 426(2):243–258.

[39] Thaler, J.P., Choi, S.J., Sajan, M.P., Ogimoto, K., Nguyen, H.T., Matsen, M., et al., 2009 Dec. Atypical protein kinase C activity in the hypothalamus is required for lipopolysaccharide-mediated sickness responses. Endocrinology 150(12):5362–5372.

[40] Schwartz, E.A., Zhang, W.-Y., Karnik, S.K., Borwege, S., Anand, V.R., Laine, P.S., et al., 2010 Apr. Nutrient modification of the innate immune response: a novel mechanism by which saturated fatty acids greatly amplify monocyte inflammation. Arteriosclerosis, Thrombosis, and Vascular Biology 30(4):802–808.

 © 2017 The Authors. Published by Elsevier GmbH. This is an open access article under the CC BY-NC-ND license (http://creativecommons.org/licenses/by-nc-nd/4.0/).

[41] Arboleda, G., Morales, L.C., Benítez, B., Arboleda, H., 2009 Mar. Regulation of ceramide-induced neuronal death: cell metabolism meets neurodegeneration. Brain Research Reviews 59(2):333–346.

[42] Kahn, B.E., Brannigan, R.E., 2017 Sep. Obesity and male infertility. Current Opinion in Urology 27(5):441–445.

[43] Kiba, T., 2004 Aug. Relationships between the autonomic nervous system and the pancreas including regulation of regeneration and apoptosis: recent developments. Pancreas 29(2):e51–58.

[44] N'Guyen, J.M., Magnan, C., Laury, M.C., Thibault, C., Leveteau, J., Gilbert, M., et al., 1994 Oct 1. Involvement of the autonomic nervous system in the in vivo memory to glucose of pancreatic beta cell in rats. Journal of Clinical Investigation 94(4):1456–1462.

[45] Leon-Quinto, T., Magnan, C., Portha, B., 1998 Aug. Altered activity of the autonomous nervous system as a determinant of the impaired β-cell secretory response after protein-energy restriction in the rat. Endocrinology 139(8): 3382–3389.

[46] Leloup, C., Orosco, M., Serradas, P., Nicolaïdis, S., Pénicaud, L., 1998 Jun 15. Specific inhibition of GLUT2 in arcuate nucleus by antisense oligonucleotides suppresses nervous control of insulin secretion. Molecular Brain Research 57(2):275–280.

[47] Parton, L.E., Ye, C.P., Coppari, R., Enriori, P.J., Choi, B., Zhang, C.-Y., et al., 2007 Sep 13. Glucose sensing by POMC neurons regulates glucose homeostasis and is impaired in obesity. Nature 449(7159):228–232.

[48] Zheng, H., 2005 Mar 10. Brain stem melanocortinergic modulation of meal size and identification of hypothalamic POMC projections. American Journal of Physiology – Regulatory, Integrative and Comparative Physiology 289(1): R247–R258.

[49] Ramírez, S., Gómez-Valadés, A.G., Schneeberger, M., Varela, L., Haddad-Tóvolli, R., Altirriba, J., et al., 2017 Jun. Mitochondrial dynamics mediated by mitofusin 1 is required for POMC neuron glucose-sensing and insulin release control. Cell Metabolism 25(6), 1390–1399.e6.

[50] Parra, V., Eisner, V., Chiong, M., Criollo, A., Moraga, F., Garcia, A., et al., 2008 Jan 15. Changes in mitochondrial dynamics during ceramide-induced cardiomyocyte early apoptosis. Cardiovascular Research 77(2):387–397.

 © 2017 The Authors. Published by Elsevier GmbH. This is an open access article under the CC BY-NC-ND license (http://creativecommons.org/licenses/by-nc-nd/4.0/).